Comparing float pCO$_2$ profiles in the Southern Ocean to ship data reveals discrepancies

Chuqing Zhang[1], Yingxu Wu[2], Peter J. Brown[3], David Stappard[1], Amavi N. Silva[1], and Toby Tyrrell[1]

[1]University of Southampton, National Oceanography Centre Southampton, Southampton, UK
[2]Polar and Marine Research Institute, Jimei University, Xiamen, China
[3]National Oceanography Centre, Southampton, UK

Correspondence to: Chuqing Zhang (Chuqing.Zhang@soton.ac.uk)

Abstract. The Southern Ocean plays a crucial role in the global carbon cycle. Recently, the utilization of biogeochemical (BGC) Argo float data has provided valuable insights into the uptake and release of carbon dioxide (CO$_2$) by this region. However, significant uncertainty remains regarding the accuracy of pCO$_2$ (partial pressure of CO$_2$) values derived from float data. In this study, we compared pCO$_2$ estimates obtained from float pH data with those from ship-collected data across the Southern Ocean, employing pCO$_2$-depth, pCO$_2$-O$_2$ and CO$_2$-O$_2$ vs saturation plots to assess the degree of agreement between these two datasets. Our findings reveal significant systematic differences. A preliminary analysis, ignoring other factors, found that the float data is consistently higher, on average, than the ship data at equivalent depths and oxygen levels. We tested the hypothesis that inaccurate float pH data or float pCO$_2$ correction process is the main cause of the pCO$_2$ difference, by quantifying other factors that could produce systematic differences, including: (i) spatial sampling bias, (ii) seasonal bias, (iii) errors in estimated alkalinity, (iv) errors in carbonate system constants, and (v) higher levels of anthropogenic CO$_2$ in float data. However, none of the other factors were found to be able to fully account for the discrepancies, suggesting issues with float pH data quality and/or the float pCO$_2$ correction process. Additional analysis included refinements to ship-based and float-based pCO$_2$ before intercomparison. Overall, we estimate that, in the Southern Ocean, surface pCO$_2$ from floats is biased high by, on average, at least 10 μatm.

1 Introduction

The Southern Ocean (SO) is a substantial carbon sink, capable of absorbing and storing globally-significant quantities of carbon dioxide (Rintoul, 2011), a service critical to the mitigation of global climate change. The Southern Ocean disproportionally accounts for roughly 40% of the global oceanic uptake of atmospheric CO$_2$ while accounting for only 25% of its surface area (Landschützer et al., 2015, Gruber et al., 2019). Meanwhile, upwelling in the SO also leads to the release of carbon dioxide to the atmosphere (Rae et al., 2018). Accurate calculation of CO$_2$ fluxes has profound implications for analyzing the carbon cycle and understanding carbon dynamics (Bauer et al., 2013). Typically, the flux is determined by measuring the difference in CO$_2$ partial pressure (pCO$_2$) between surface waters and the overlaying air. Historically,

previous calculations of surface CO_2 fluxes were based on high-quality shipboard data (McNeil et al., 2007, Metzl et al., 2006, Lenton et al., 2013) but ocean measurement equipment developed in recent years has opened up new avenues for the determination of pCO_2 and CO_2 fluxes, including biogeochemical (BGC) Argo floats, aircraft, and uncrewed surface vehicles (Claustre et al., 2020, Long et al., 2021, Sutton et al., 2021). BGC floats hold great potential as an efficient tool for

35   carbon cycle research particularly in the inhospitable SO, as they can rapidly generate a substantial volume of data with broad spatial and temporal coverage, bridging gaps in the sparse shipboard observations (Johnson et al., 2017).

Up to December 2022, 493 BGC Argo floats had been deployed across the global oceans, (https://www.go-bgc.org/array-status#current-deployments), equipped with biological and chemical sensors to measure a combination of oxygen (O_2), nitrate, pH and other variables over a lifespan of several years (Owens et al., 2022). Measurements (vertical profiles) are

40   made every 5-10 days and the resulting data is useful for investigation of marine biogeochemical processes, including ocean acidification, carbon cycling, and air-sea gas exchange (Matsumoto et al., 2022). As pCO_2 is not currently measured directly, it is estimated using a combination of float-measured pH and algorithm-estimated total alkalinity (TA) (Bushinsky et al., 2019, Williams et al., 2017). When float-based estimates of pCO_2 are incorporated into large-scale estimates of carbon flux in SO, substantial disparities in the magnitude of the flux have been revealed compared to those estimates derived solely

45   from ship-based measurements or from non-marine data (Long et al., 2021, Gray et al., 2018, Bushinsky et al., 2019). Using solely BGC float data, an annual CO_2 flux of -0.08 Pg C/yr was calculated by Gray et al. (2018), while combining with ship data led to an annual mean Southern Ocean (south of 35°S) sink of -0.35 ± 0.19 Pg C/yr being calculated for the years 2015–2017 (Bushinsky et al., 2019). These estimates compare to a value of -1.14 ± 0.19 Pg C/yr based entirely on ship data (where negative values indicate net carbon fluxes into the ocean), meaning the annual net flux based entirely on float data is

50   considerably smaller than the value based on ship data.

What leads to this difference between float-based and ship-based CO_2 flux estimates? Bushinsky et al. (2019) attributed it to ships lacking data from winter observations (when pCO_2 values are the highest) at high Antarctic latitudes. However, Mackay and Watson (2021) found their estimates of winter outgassing (extrapolated from summertime ship observations) to be much smaller than the float-derived observations and close to long-term ship data estimation results. Moreover, Long et al.

55   (2021) calculated the ocean-atmosphere CO_2 flux using data collected from aircraft and found it to be close to the ship-based CO_2 flux but to significantly different from the float-based CO_2 flux (aircraft-based annual mean flux for 2009–2018 of -0.53 $\pm$ 0.23 Pg C/yr, compared to float annual mean of around +0.3 Pg C/yr for 2015–2017) in south of 45°S. Furthermore, Wu and Qi (2023) highlight the no seasonal difference throughout the year feature of CO_2 flux difference between float-based and ship-based, which could not be explained by the hypothesis Bushinsky et al. (2019) proposed. These results raise the

60   possibility that the difference in CO_2 fluxes may stem from the calculation of pCO_2 from float pH data.

A fundamental challenge associated with BGC float pH data is the limited opportunity for maintenance and servicing once deployed in the ocean, despite potential exposure to various contaminants and risks of damage during their extended lifetime of oceanic measurements. Factors such as bio-detritus deposition can introduce biases into the collected float data (Bittig et al., 2019, Claustre et al., 2020). In contrast, equipment used for acquiring ship-based data undergoes frequent and repeated

65 maintenance, field testing, and calibration and is thus generally considered to be more reliable than float-derived data (Pierrot et al., 2009, Williams et al., 2017).

Williams et al. (2017) identified a large number of potential sources of float pCO_2 uncertainty, which they grouped into 3 categories: (1) uncertainties in pH sensors, (2) uncertainties in derived alkalinity estimates, and (3) uncertainties in carbonate system equilibrium constants, with (1) having the greatest contribution. Although there is a quality control and calibration

70 process applied to float pH data, including linear drift correction and crossover comparison (with co-located ship data) correction (Maurer et al., 2021), questions still remain regarding the calibration process and its outputs (Wu et al., 2022, Álvarez et al., 2020, Huang et al., 2023). Álvarez et al. (2020) highlighted the mismatch between float-based and ship-based pH values. Mackay and Watson (2021) reconstructed winter pCO_2 data based on ship-collected summer data, and found them to diverge somewhat from the float pH data based pCO_2. Sutton et al. (2021) concluded that float pCO_2 data exhibit

75 greater uncertainty than ship and uncrewed surface vehicle-collected pCO_2 data. Moreover, Wu et al. (2022) employed an integrated analysis of carbon dioxide and oxygen concentrations which identified data offsets in float pH and derived pCO_2 data. Wu and Qi (2022) revealed an inconsistency between ship and BGC float-based pCO_2 in the Drake Passage region. Wimart-Rousseau et al. (2023) scrutinized the existing float pH correction process and found it insufficient, suggesting that a second reference point nearer to the surface would improve estimates.

80 Given the questions raised by these studies, a basin-scale quantitative examination of differences between float based pCO_2 and ship-based (Global Data Analysis Project: GLODAP) pCO_2 data proposed. Here we present the results of such a comparison in the SO. We apply various analytical tools such as pCO_2 vs. depth plots, pCO_2 vs. O_2 plots and plots which compare coupled deviations of CO_2 and O_2 concentrations from saturation (CORS plots as proposed by Wu et al. (2022)) to identify any discrepancies between the two datasets across 0-2000 m. Our analysis accounts for several factors that could

85 potentially affect these differences, ultimately concluding that issues with float pH data quality and its use for calculating pCO_2 contributed at least in part to the observed discrepancies.

2 Materials and Methods

2.1 Data sources

In this study, we focus on the SO delineated south of 50°S latitude, following Wu et al. (2022), and the surface layer is

90 defined as depths shallower than 100m, due to the deeper mixed layers in this region (Dong et al., 2008). We utilised comprehensive datasets comprising both float (over 300,000 sampling points) and ship (over 30,000 sampling points) measurements collected within the region (Fig. 1).
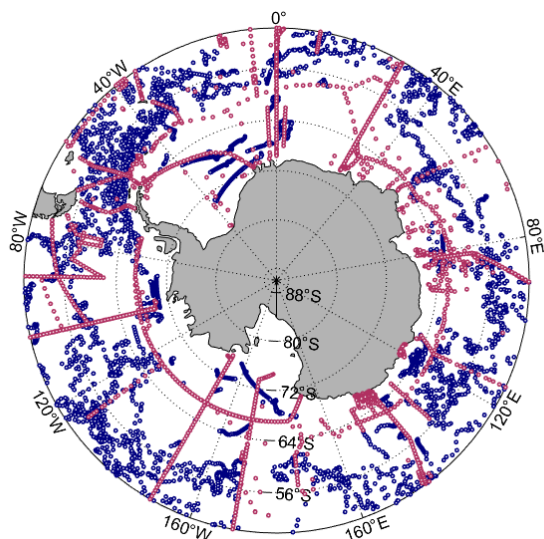
Figure 1. Location of ship data (red) and float data (blue) in the SO region.

2.1.1 BGC Argo float data

The BGC Argo data (NetCDF formatted version, accessed on 02 April 2023) were downloaded from https://data-argo.ifremer.fr/. We used "MATLAB toolbox for accessing and visualizing Argo data" (Frenzel, 2022) to select all 275 floats that entered the SO region in the period 2014 to 2023. The final float data (Matlab formatted version) used in this research includes: ID, longitude, latitude, depth, date, temperature, salinity, pH(in-situ), nitrate, oxygen and quality control flags of pH(in-situ), nitrate, oxygen. All the BGC Argo data used in this study was delayed mode (calibrated by the Argo Global Data Assembly, Centers GDAC). The quality control (QC) flag value of "1" for the BGC Argo floats means that data quality is good according to the GDAC. Only the data where all of nitrate (to calculate TA), oxygen and pH had a QC flag of "1" were selected for our research (Schmechtig and Thierry, 2016).

2.1.2 GLODAP (ship) data

The GLODAP (ship) data were obtained from (https://www.glodap.info, last access: 05 October 2022). The GLODAPv2.2022 dataset contains almost 1.4 million internally-consistent samples of biogeochemical variables globally, collected on 1085 cruises during the period 1972–2021 (Lauvset et al., 2022). The final ship data used in this research includes: longitude, latitude, depth, date, temperature, salinity, dissolved inorganic carbon (DIC), TA, oxygen, silicate, phosphate and respective World Ocean Circulation Experiment (WOCE) flags. The WOCE flags were an indication of whether the corresponding data is reliable. Only bottles where all of DIC, TA and oxygen were acceptable (WOCE flag 2) were selected for our research (Lauvset et al., 2021).

2.2 pCO$_2$ calculations

The MATLAB v3.1.2 of CO2SYS (Van Heuven et al., 2011, Sharp, 2023) was used to calculate pCO$_2$ using the carbonate system constants of Lueker et al. (2000), to ensure consistency with the previous studies (Williams et al., 2017, Bushinsky et al., 2019, Gray et al., 2018).For the ship data, pCO$_2$ was calculated from DIC and TA. For float data, pCO$_2$ was calculated from measured pH and algorithm-estimated TA. For the float data, the data processing was therefore divided into two steps: (1) estimation of TA and, (2) calculation of pCO$_2$ from estimated TA and observed pH (Williams et al., 2017). TA was estimated using the LIAR algorithm (Carter et al., 2018). We supplied the LIAR algorithm with the 3 necessary inputs: longitude, latitude and depth, and 4 additional parameters measured by the floats: temperature, salinity, nitrate and oxygen. The values of silicate and phosphate have a negligible effect on the calculation of pCO$_2$ from pH and TA (Williams et al., 2017) and were always entered as zero for float pCO$_2$ calculations. For ship pCO$_2$ calculations (pCO$_2$ from DIC and TA), on the other hand, silicate and phosphate have non-negligible effects and were taken from GLODAP data files (Lueker et al., 2000).

The float pH data recommended for researchers undergoes a calibration procedure at the data center: for each profile, the pH measured by the float at a depth of 1500, is compared to an expected value calculated from ship data. As properties are assumed to remain relatively constant over time, any pH difference detected is subtracted from the entire float profile (Maurer et al., 2021). The pH correction process for floats should result in a more accurate alignment between float and ship pCO$_2$ at depths below 1500 meters, as compared to data at other depths. The float pH data we used had been corrected in this way.

An additional adjustment is recommended when calculating pCO$_2$ from float pH (Williams et al., 2017) , that we applied is summarize thus: (1) float measured pH (in-situ) is converted to pH (25°C, 0 dbar). (2) Using equation (1) and the 1500m pH (25°C, 0 dbar), a correction is calculated for each profile. (3) This is added to each pH value in the profile before finally calculating pCO$_2$.

$$pH\ adjustment = -0.034529 \times pH(25°C) + 0.26709 \quad (1)$$

2.3 Approaches for interrogating differences in pCO$_2$

Three approaches were employed to investigate the disparity between float pCO$_2$ and ship pCO$_2$: pCO$_2$-depth plots, pCO$_2$-O$_2$ plots and CORS plots. The pCO$_2$-depth plot effectively illustrates systematic variations across the entire profile, making it an ideal method for elucidating differences in pCO$_2$ at different depths. The pCO$_2$-O$_2$ plots and CORS plots are based on the biogeochemical relationship between CO$_2$ and O$_2$. Previous research has demonstrated that oxygen sensor data from floats has the highest rate of 'good' data return (100%) while the pH sensors have a lower rate of good data return (88%) (Johnson et al., 2017). In crossover comparisons with GLODAPv2, the oxygen data measured by floats was found to exhibit a strong correlation with the corresponding GLODAPv2 ship-derived data, displaying a consistent 1:1 relationship (Johnson et al., 2017). However float pH data exhibited notable deviations from GLODAPv2 data, and the expected 1:1 relationship

(Johnson et al., 2017, Huang et al., 2023), with the addition of anthropogenic CO_2 in surface suggested as a potential cause.

145 Given that float-measured O_2 data exhibits a higher likelihood of accuracy compared to float-derived pCO_2, it is not affected by ocean acidification-related effects, and that they are both simultaneously involved in many processes (gas exchange, photosynthesis, respiration), O_2 data from floats can serve as a robust constraint for checking float pCO_2 values.

Taking into account the significant influence of surface pCO_2 on air-sea fluxes and the use of data from 1500 m in the calibration process, we calculated two metrics of particular interest: (1) the mean difference in pCO_2 values at the surface

150 (averaging over all data from 0 - 100 m, referred to as $\Delta pCO_{2, Surface}$) and (2) the mean difference in pCO_2 values in the deep ocean (averaging over all data from 1500-2000 m, referred to as $\Delta pCO_{2, DeepOcean}$).

2.3.1 pCO_2-depth

We use ship-float pCO_2 data comparisons between surface (depths <100m) and deep (1500-2000 m) waters to qualitatively assess the degree of overlap and deviation, with outputs binned into 100 m vertical intervals to examine depth-dependent

155 differences.

2.3.2 pCO_2-O_2

Similarly, we compare pCO_2 outputs against in situ oxygen levels, binning outputs into 10 μmol/kg oxygen intervals to examine potential disparities between them.

2.3.3 Carbon and oxygen relative to saturation (CORS)

160 The CORS method is an improved CO_2-O_2 analysis technique which involves comparing the deviations of O_2 and CO_2 concentrations to their respective saturation levels. Following Wu et al. (2022), we adopted an identical approach for both O_2 and CO_2 and proceeded to compare the dissolved concentrations of O_2 and CO_2 ([O_2] and [CO_2] respectively) in surface seawater with their respective saturation values. The saturation values represent the points at which the net air-sea gas exchange rate would be zero for each gas. Differences from saturation are calculated following:

165
$$\Delta O_2 = [O_{2,observed}] - [O_{2,saturation}] \quad (2)$$

$$\Delta CO_2 = [CO_{2,observed}] - [CO_{2,saturation}] \quad (3)$$

The saturation concentration of O_2 was calculated using Garcia & Gordon's equation (Garcia and Gordon, 1993, Garcia and Gordon, 1992); however, while they calculated the O_2 saturation concentration at an assumed 1 atm of atmospheric pressure, we instead used the local in-situ sea level pressure (SLP, usually < 1 atm in the SO) as per the below:

170
$$[O_{2,saturation}^{1atm}] = K \times pO_2^{1atm} = K \times xO_{2,air} \times (P_{1atm} - P_{Sw}) \quad (4)$$

$$[O_{2,saturation}^{SLP}] = K \times pO_2^{SLP} = K \times xO_{2,air} \times (P_{SLP} - P_{Sw}) \quad (5)$$

Here, the '1atm' and 'SLP' indicate two different pressures. K is the solubility of oxygen, $O_{2,saturation}^{1atm}$ is the result based on the Garcia & Gordon's equation (Garcia and Gordon, 1993, Garcia and Gordon, 1992). $O_{2,saturation}^{SLP}$ is the result based on

our modified equation. P_{Sw} is the water vapor pressure calculated from the surface temperature and salinity (Weiss and Price,

175 1980b). P_{SLP} is taken from the monthly gridded climate data downloaded from National Oceanic and Atmospheric Administration (NOAA) (Gridded Climate: NOAA Physical Sciences Laboratory, last access: 10 July 2022). Combining equations (4) and (5):

$$[O_{2,saturation}^{SLP}] = [O_{2,saturation}^{1atm}] \times (P_{SLP} - P_{Sw})/(P_{1atm} - P_{Sw}) \ (6)$$

$[CO_{2,saturation}]$was calculated with Henry's equation. ($[CO_{2,observed}] = K_H \times pCO_{2,equilibrium}$), where $pCO_{2,equilibrium}$ is

180 the partial pressure of CO_2 in seawater at equilibrium with atmospheric CO_2; it was calculated according to the equation:

$$pCO_{2,equilibrium} = xCO_{2,air} \times (P_{SLP} - P_{Sw}) \ (7)$$

where the $xCO_{2,air}$ is the mole fraction of carbon dioxide (ppm) in dry atmosphere. The monthly mean atmospheric $xCO_{2,air}$ values from the monitoring site at Palmer Station, Antarctica were used for the SO (downloaded from https://www.esrl.noaa.gov/gmd/ccgg/trends/, last access: 14 July 2022). The solubility (K_H) of carbon dioxide is calculated

185 from the formula proposed by Weiss (1974).

3 Results

3.1 pCO_2 differences at different depths

Initially, scatter plots were generated to compare the pCO_2 data obtained from floats and ships at different depths. Fig.2 shows a difference between the pCO_2 values derived from the floats and those acquired from the ships. Generally, the ship

190 data and float data exhibit a substantial overlap, although a fraction of the float data has higher pCO_2 values than the ship data from the same depths.
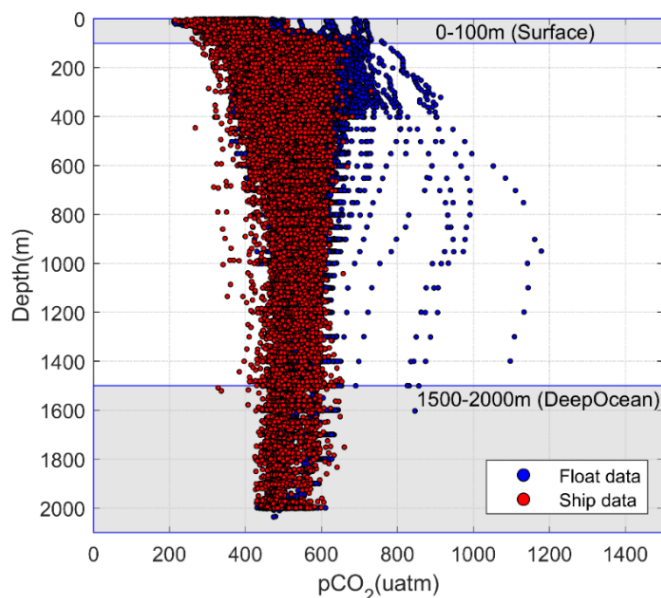
Figure 2: Scatterplot of $p\mathrm{CO_2}$ at different depths in the Southern Ocean. Float data (blue) is plotted first and ship data (red) second (Supplement Fig. S1 shows the same plot but with ship data plotted first).

195 The mean difference plot (Fig. 3) reveals two notable observations. Firstly, the $p\mathrm{CO_2}$ values derived from the float data are, on average, higher than the ship data at most depths. Secondly, the discrepancy between the float and ship data is particularly pronounced at depths shallower than 1500 m.
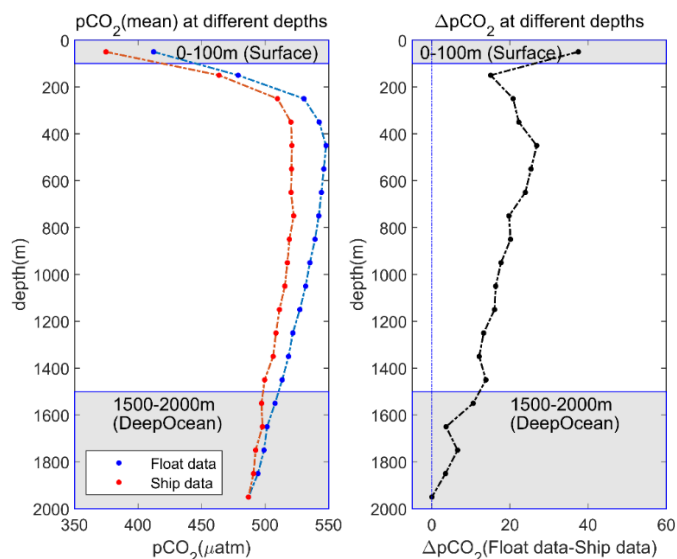

Figure 3: $p\mathrm{CO_2}$(mean) at different depths. The left panel shows the average float and ship $p\mathrm{CO_2}$ at different depths; the right
200 panel shows the difference between the two (float $p\mathrm{CO_2}$ minus ship $p\mathrm{CO_2}$).

The values of the two metrics of particular interest (section 2.3) are $\Delta p\mathrm{CO_{2,Surface}} = 37.5$ µatm and $\Delta p\mathrm{CO_{2,DeepOcean}} = 4.9$ µatm. These act as benchmarks for later analysis and discussion. As is apparent in Fig. 2, some float data points exhibit unusually high $p\mathrm{CO_2}$ values (over 750 µatm), despite being corrected and marked as good by the GDAC. We checked for the effect of removing these possibly anomalous data; however, because we were not certain that the data are incorrect, and because their
205 removal had minimal effect on the $p\mathrm{CO_2}$ averages (no more than 0.1 µatm), we did not exclude them from our analyses and plots.

3.2 $p\mathrm{CO_2}$ differences from $p\mathrm{CO_2}$-oxygen relationships

$\mathrm{O_2}$ increases/decreases are often accompanied by $p\mathrm{CO_2}$ decreases/increases because of photosynthesis and respiration, leading to a negative correlation between the two (Fig. 4). Here, it is evident that while the $\mathrm{O_2}$ values exhibit similarity, the
210 $p\mathrm{CO_2}$ derived from float data demonstrates an overall higher magnitude in parameter space than that obtained from ship data.

8

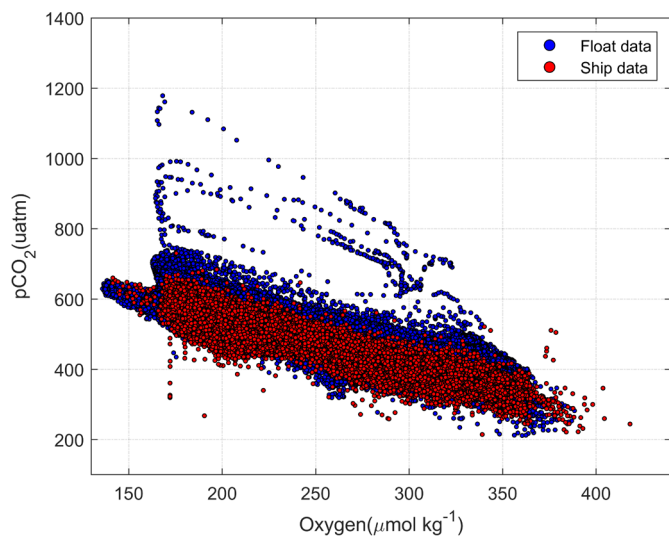**Figure 4:** Scatterplot of pCO$_2$ against oxygen (ship data and float data) in the SO region. (Float data (blue) is plotted first and ship data (red) second (Supplement Fig. S2 shows the same plot but with ship data plotted first, to avoid the effects of masking)

215 We further calculated the average pCO$_2$ values within different oxygen intervals (ranging from 150 to 360 μmol/kg) and examined the differences between them (Fig. 5). The average pCO$_2$ difference was calculated to be 19.3 μatm (obtained by subtracting ship data from float data). Our analyses indicate a consistent and significant systematic disparity between the pCO$_2$ values obtained from float data and ship data, with consistently higher float pCO$_2$ values within each oxygen interval.
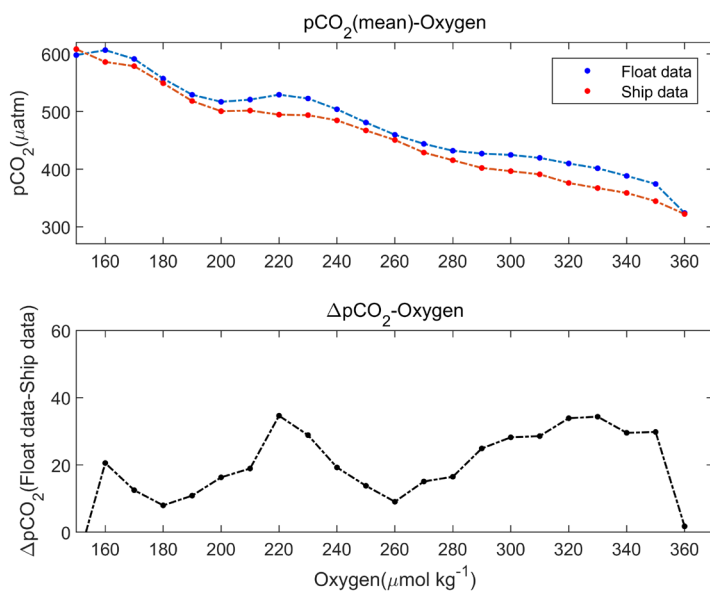
220 **Figure 5:** pCO_2 (mean) against oxygen of float and ship data (above); the difference (ΔpCO_2, below) is calculated as float pCO_2 minus ship pCO_2.

3.3 CORS plots of ship data and float data

Fig. 6 shows a CORS plot of both ship data and float data from the Southern Ocean. The pattern of float data is comparable to that of ship data: a large number of data points are situated in the top-left quadrant, i.e., supersaturation of CO_2 along with

225 undersaturation of O_2. This pattern can be attributed to upwelling of CO_2-rich and oxygen-poor deep waters, where the deep-water composition has been changed by remineralization of sinking organic matter.
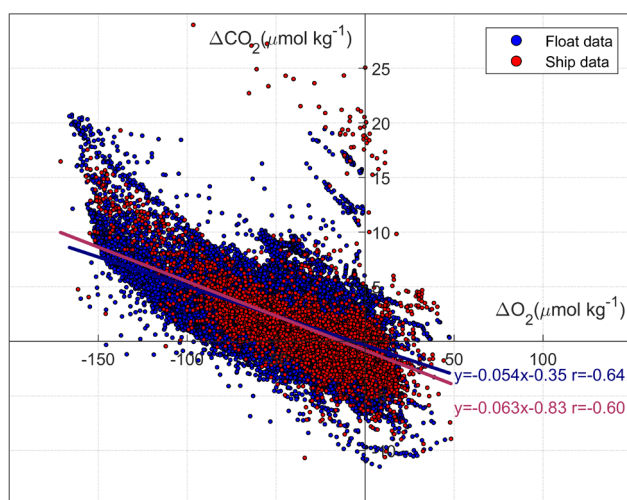
Figure 6: CORS plot from surface float data (blue) and ship data (red). The blue line is the best-fit line to float data and the pink line is the best-fit line to ship data. r is the associated Pearson correlation coefficient. Float data (blue) is plotted first

230 and ship data (red) second, masking the locations of many float data.

In situations where biogeochemical and physical processes like photosynthesis and upwelling strongly influence the system, the deviations of O_2 and CO_2 from atmospheric equilibrium demonstrate a coupled behavior, as photosynthesis and remineralization affect carbon and oxygen in contrasting directions, according to a stoichiometric ratio. We find different CORS plot y-intercepts for float data and for ship data (Fig 6): the ship data based y-intercept is –0.83 μmol kg^{-1}, while the

235 float data based y-intercept is -0.35 μmol kg^{-1}, a difference of 0.48 μmol kg^{-1} (float data minus ship data). Converting the offset in [CO_2] (μmol kg^{-1}) to pCO_2 (μatm), assuming average values for sea surface temperature (1°C) and salinity (35), gives a mean difference in surface pCO_2 of 7.7 μatm.

4 Discussion

The results in Fig. 3, Fig. 5 and Fig. 6 show a notable disparity between pCO_2 values derived from float data and those
240 obtained from ship data. We now examine potential causes of the differences other than data error. There are several factors
that could potentially influence the differences in pCO_2 values: (i) spatial sampling bias between the two databases, (ii)
seasonal bias in the ship-collected data, (iii) errors in estimated alkalinity, (iv) errors in carbonate system constants, and (v)
higher levels of anthropogenic CO_2 in float data. Only by excluding these factors can we conclude that the observed
deviation in pCO_2 is likely to be due to problems with the quality of the pCO_2 data from the floats.

245 ### 4.1 Impact of different factors on disparities

4.1.1 Spatial sampling bias between two databases

To exclude the potential impact of sampling area variations, we compare float-measured pCO_2 and ship-measured pCO_2 data
within specific regions. In particular, we focus on the Drake Passage region (55°S to 65°S, 55°W to 70°W) as a
representative case study (Fig. 7) (Wu and Qi, 2022, Wu et al., 2022). Comparing data only from within this specific region
250 (where there are large amounts of both ship and float data) excludes any confounding effects arising from variations in
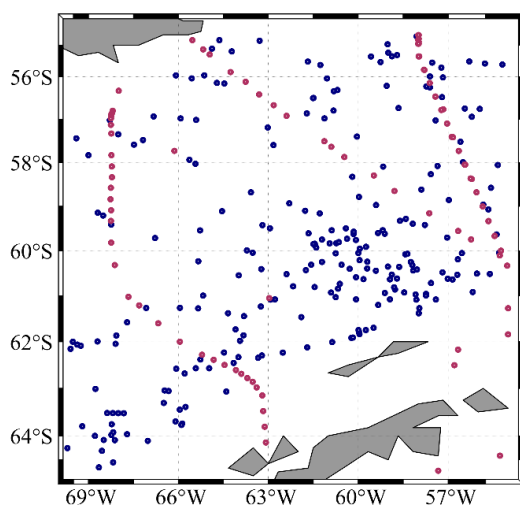sampling locations.

Figure 7: Location of ship data (red) and float data (blue) in the Drake Passage region.

In line with our analysis of the complete dataset encompassing the Southern Ocean, we computed the average pCO_2 values at
255 various depths. Within the Drake Passage region (1166 ship data points and 16137 float data points) we observed a
$\Delta pCO_{2,Surface}$ value of 37.2 µatm, accompanied by a $\Delta pCO_{2,DeepOcean}$ value of -16.8 µatm (Fig. 8), compared to 37.5 and 4.9
µatm for the SO as a whole (section 3.1). A similar analysis in the region around the prime meridian, near Antarctica (70°S-
65°S, 10°W-10°E) (1226 ship data points and 6818 float data points), produced $\Delta pCO_{2,Surface}$ = 45.4 µatm and $\Delta pCO_{2,DeepOcean}$

= 1.7 µatm (Supplement Fig. S3 and S4). The persistence of substantial differences in both regions indicates that spatial

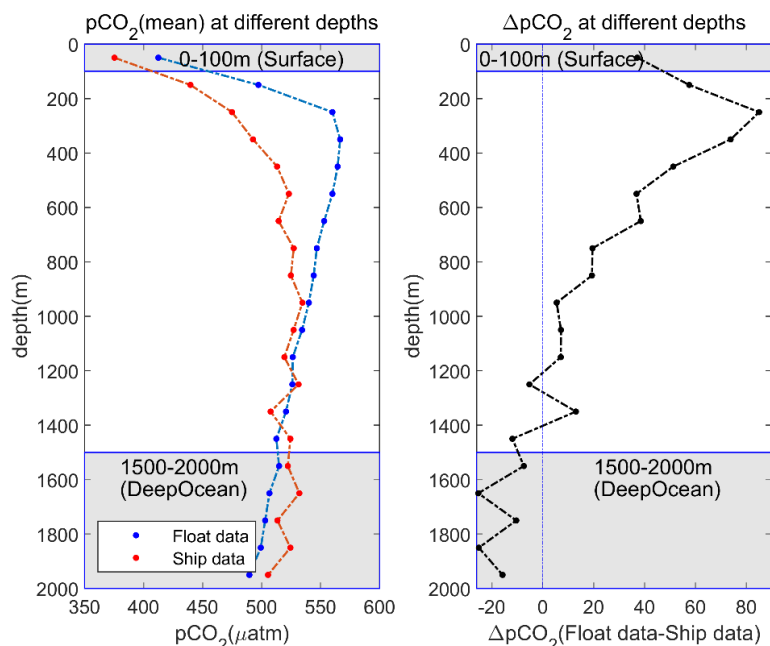260 variability alone does not entirely account for the disparities in pCO_2 between the two datasets.

Figure 8: pCO_2 (mean) at different depths (left), and difference between float pCO_2 minus ship pCO_2 at different depths (right) in Drake Passage region.

4.1.2 Seasonal bias in ship data

265 To mitigate the potential influence of sparse winter sampling conducted by ships, we carefully assessed the distribution of ship data across different months (Supplement Fig. S5). Float data is evenly distributed over the seasons, while ship data is mainly concentrated in summer. Consequently, we specifically selected ship and float data from November to April, omitting winter data (May to October) from both datasets. This eliminated the possible confounding effect of seasonal variations in sampling intensity. The resulting average differences in pCO_2 values are $\Delta pCO_{2,\text{Surface}}$ = 32.4 µatm and

270 $\Delta pCO_{2,\text{DeepOcean}}$ = 6.6 µatm. $\Delta pCO_{2,\text{Surface}}$ is reduced by 5.1 µatm, while $\Delta pCO_{2,\text{DeepOcean}}$ is increased by 1.7 µatm. By removing seasonal bias, we were able to slightly reduce the sea surface pCO_2 difference, but the finding of an overall higher pCO_2 in the floats did not change.

4.1.3 Errors in estimated alkalinity

In order to examine the difference between TA estimated from float data and TA measured from ships, the average

275 difference at different depths between float TA and ship TA was calculated in the same way as for pCO_2 data. TA from ships was on average 3.6 µmol kg^{-1} higher than TA estimated from floats. This offset was used to correct the float TA and pCO_2

was calculated again using the corrected float TA and the measured pH, yielding a new $\Delta pCO_{2,\text{Surface}}$ of 38.1 µatm and $\Delta pCO_{2,\text{DeepOcean}}$ of 5.6 µatm. Therefore, the pCO_2 differences between the two databases are not due to TA errors, confirming previous studies that reached similar conclusions (Williams et al., 2017, Gray et al., 2018, Bushinsky et al., 2019, Wu et al.,
280   2022).

4.1.4 Errors in carbonate system constants

In the calculation of pCO_2 for floats and ship, we used the Lueker et al. (2000) carbonate dissociation constants in the CO2SYS program. Some recent work has shown that current estimates of the carbonate system constants appear inaccurate in cold ocean regions (Woosley and Moon, 2023, Sulpis et al., 2020). We recalculated the pCO_2 values with two other sets of
285   constants, Sulpis et al. (2020) and Roy et al. (1993). With Sulpis et al.'s constant, the updated $\Delta pCO_{2,\text{Surface}}$ value of 39.7 µatm and $\Delta pCO_{2,\text{DeepOcean}}$ value of 7.3 µatm reflect a slightly increase, while, conversely, employing Roy et al.'s constants yielded a new $\Delta pCO_{2,\text{Surface}}$ value of 31.5 µatm and $\Delta pCO_{2,\text{DeepOcean}}$ value of -2.0 µatm, a reduction in both variables. It is evident from the findings that employing different carbonate system constants in the calculations can alter the differences. However, neither set removes the significant discrepancy between ship and float pCO_2 values. In order to ensure consistency
290   and enable meaningful comparisons with previous studies, we have used Lueker et al.'s (2000) constants as the chosen carbonate system constants throughout the rest of this study.

4.1.5 Higher levels of anthropogenic CO₂ in float data

The pCO_2 in the ocean responds to the rising trends in atmospheric carbon dioxide concentrations due to the burning of fossil fuels (Bates et al., 2014). Float data has, on average, been collected more recently than ship data, and so the water the floats
295   sampled can be expected to contain higher levels of anthropogenic CO_2 (Supplement Fig. S6). To prevent temporal pCO_2 trends being mistaken for discrepancies, we normalized both float and ship surface pCO_2 to the reference year of 2005, where "surface data" is defined as data collected in the uppermost 100m (de Boyer Montégut et al., 2004). The normalization is based on assuming that surface pCO_2 tracks atmospheric pCO_2(Feely et al., 2008, Wu et al., 2019). First, we calculated the variation in the molar fraction of CO_2 in the atmosphere ($xCO_{2,\text{air}}$) from the reference year 2005 to the year of data collection.

300
$$\Delta xCO_{2,air} = xCO_{2,air}^{Year} - xCO_{2,air}^{2005} \quad (8)$$

where the superscript "Year" refers to the year of data collected and the superscript "2005" refers to the reference year. The globally annual average $xCO_{2,\text{air}}$ data was downloaded from (https://www.esrl.noaa.gov/gmd/ccgg/trends/, last access: 18 April 2023). We used mean values of float in-situ surface ocean temperature (T) and salinity (S) data to calculate humidity (pH₂O) data (Weiss and Price, 1980a),

305
$$\ln pH_2O = 24.4543 - 67.4509 \left(\frac{100}{T}\right) - 4.8489 \ln \left(\frac{T}{100}\right) - 0.000544 S \quad (9)$$

then converted $\Delta xCO_{2,\text{air}}$ into $\Delta pCO_{2,\text{air}}$ (Takahashi et al., 2014, Weiss and Price, 1980a).

$$\Delta pCO_{2,air} = \Delta xCO_{2,air} \times (1 - pH_2O) \quad (10)$$

13

Based on the assumption that $\Delta pCO_{2,\text{surface}}$ is equal to $\Delta pCO_{2,\text{air}}$, the surface $pCO_{2,\text{surface}}$ normalized to reference year 2005 was calculated as

$$pCO_{2,surface}^{2005} = pCO_{2,surface}^{Year} - \Delta pCO_{2,surface} = pCO_{2,surface}^{Year} - \Delta xCO_{2,air} \times (1 - pH_2O) \quad (11)$$

where $pCO_{2,surface}^{Year}$ is the in-situ pCO_2 at the time of data collection, whether by float or ship. After normalization of the sea surface pCO_2 data, the new $\Delta pCO_{2,\text{Surface}}$ is 13.1μatm and $\Delta pCO_{2,\text{DeepOcean}}$ is still 4.9μatm. The temporal pCO_2 trends and the ongoing accumulation of anthropogenic CO_2 in surface waters can thus explain a sizeable portion of the difference but does not eliminate it completely.

4.2 Adjusted pCO_2 differences after taking multiple factors into account

Each of these factors individually influenced the variance results to some degree, but none can independently fully explain the observed differences in pCO_2 (Table 1). However, it is worth considering whether the inclusion of all of these influences together would yield a different result. Since the spatial bias (4.1.1) was obtained by separately calculating the data for the different regions, we do not include it here in the adjustment to the Southern Ocean data, but rather as a separate control analysis. For carbonate system constants (4.1.4), the discrepancies either increase or decrease depending on which alternative set of constants is used, and we decided to stay with the constants of Lueker et al. (2000) in order to maintain consistency with other studies. Therefore, no correction was made for this. Here we take the seasonal bias (4.1.2), errors in estimated TA (4.1.3), and anthropogenic CO_2 influence (4.1.5) into account and recalculate the pCO_2 differences.

Table 1

Possible reasons for the pCO_2 discrepancies and their magnitudes after calculations to exclude their influence (changes in value from the initial analysis are shown in brackets).

| Possible reasons of observed pCO_2 discrepancy	$\Delta pCO_{2,DeepOcean}$ (after adjustment)	$\Delta pCO_{2,Surface}$ (after adjustment)
Initial analysis (no adjustments)	**4.9**	**37.5**
1. Spatial sampling bias between two databases (top line Drake Passage, bottom line region around the prime meridian)	-16.8 (-21.7) μatm/ 1.7 (-3.2) μatm	37.2 (-0.3) μatm/ 45.4 (+7.9) μatm
2. Seasonal bias in ship-collected data	6.6 (+1.7) μatm	32.4 (-5.1) μatm
3. Errors in estimated alkalinity	5.6 (+0.7) μatm	38.1 (+0.6) μatm
4. Errors in carbonate system constants (top line Sulpis et al., 2002; bottom line Roy et al., 1993)	7.3 (+2.4) μatm/ -2.0 (-6.9) μatm	39.7 (+2.2) μatm/ 31.5 (-6.0) μatm
5. Higher levels of anthropogenic CO_2 in float	-	13.1 (-24.4) μatm

14

data (surface only)		
2, 3 & 5 combined	**7.4** (+2.5) µatm	**9.4** (-28.1) µatm

330

Excluding seasonal, alkalinity and anthropogenic CO_2 effects results in updated estimates of $\Delta pCO_{2,DeepOcean}$: 7.4 µatm, and $\Delta pCO_{2,Surface}$: 9.4 µatm (Fig. 9). The adjusted average difference between the various oxygen intervals was calculated to be 10.0 µatm (Supplement Fig. S7). In the case of CORS plots, considering that ΔCO_2 is the difference between the observed concentrations relative to the saturated concentration at the time of sampling, normalizing the pCO_2 to year 2005 isn't required. Here we take the factors 2 & 3 (from Table 1) into account when constructing an adjusted CORS plot. The final y-axis intercept difference is 0.40 µmol kg^{-1}. As noted above, the offset in y-intercept ($[CO_2]$, in µmol kg^{-1}) can be converted to a deviation in pCO_2 (µatm) by assuming a temperature of 1℃ and salinity of 35; doing this yields an adjusted surface pCO_2 difference of 6.4 µatm (Supplement Fig. S8).
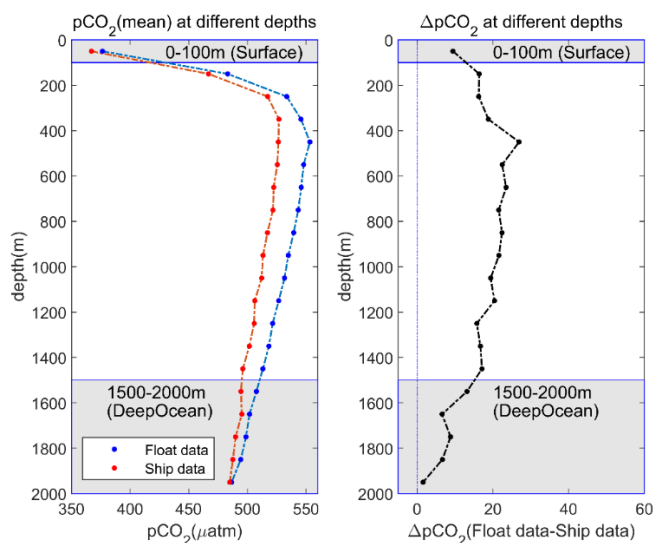
Figure 9: Adjusted pCO_2 (mean) (incorporating factors 2, 3 & 5 in Table 1) at different depths (left), and difference between float pCO_2 minus ship pCO_2 at different depths (right) in the SO.

4.3 Evaluation by comparison to SOCAT data

An alternative source of ship-collected pCO_2 data, for surface waters only, is the Surface Ocean CO_2 Atlas (SOCAT) data (Bakker et al., 2016). pCO_2 values in SOCAT are from direct measurements, believed to be highly accurate (<2 µatm) and reliable. We compared float pCO_2 to SOCAT pCO_2 in the region shown in Fig. 10 (Munro et al., 2015a). After accounting for factors 2 & 5 (Table 1), we obtained a pCO_2 discrepancy (float minus SOCAT) of 8.3 µatm. The result is close to the

discrepancy obtained from previous comparison of the float data and GLODAP data. This is strong evidence that there is inaccuracy in the float data pCO_2.
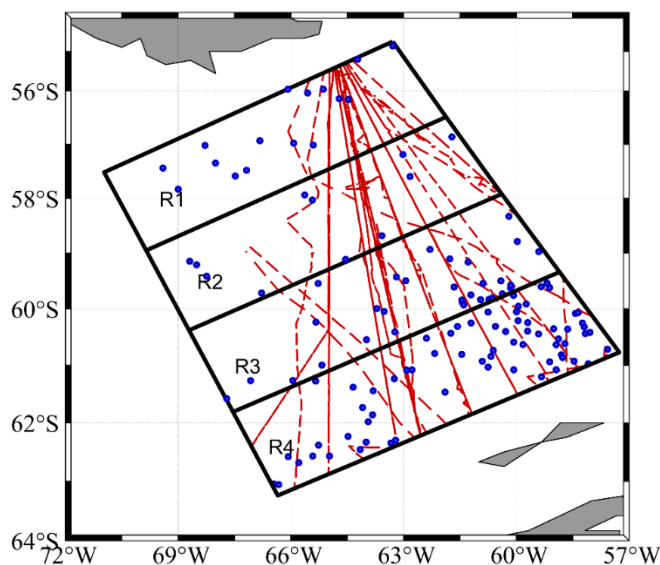
Figure 10: Location of SOCAT data (red) and float data (blue) in the Drake Passage region. The divisions R1-R4 are those used by Munro et al. (2015).

Our rigorous analysis and assessment, as summarized in Table 1: we account for several of the above factors simultaneously, and obtain a final pCO_2 difference. To determine the effects of spatial sampling bias, we apply the same analysis to specific regions as to all the SO and the discrepancy remain clear in regional analyses. To correct for seasonal bias, we subtract 5.1 µatm from surface values and add 1.7 µatm to deep values. To compensate the errors in estimated alkalinity, we add 3.6 µmol kg^{-1} to the float TA data in order to obtain the final TA value. For the anthropogenic CO_2 effect, we normalize both the ship pCO_2 and float pCO_2 to the reference year of 2005 to remove the temporal pCO_2 trends, assuming (this can only be partially correct, given the long timescales of equilibration of CO_2 in the SO (Jones et al., 2014)) that air-sea gas exchange has run to completion in all surface waters. For carbonate system constants, the discrepancies either increase or decrease depending on which alternative set of constants is used, and we decided to stay with the constants of Lueker et al. (2000) in order to maintain consistency with other studies.

4.4 Final pCO_2 differences and potential sources

Discrepancies remain even after the several possible explanatory factors (2, 3, & 5 in Table 1) were applied simultaneously to the whole of the SO. The final $\Delta pCO_{2,\text{Surface}}$ value stands at 9.4 µatm, while the final $\Delta pCO_{2,\text{DeepOcean}}$ value is 7.4 µatm. (For the factor 1, we applied the adjustement of factor 2, 3, 5 to data in Drake Passage region and region around the prime meridian, obtained the $\Delta pCO_{2,\text{Surface}}$ values are 11.4 µatm and 9.3 µatm respectively. They served as a control and are not included in the final consideration of the overall deviation of the Southern Ocean.) Lastly, we employed hypothesis testing

16

to enhance our findings. Firstly, we examined the distribution of both ship and float pCO_2 adjusted data (Supplement Fig. S9), utilizing Kolmogorov-Smirnov Testing to assess the normality of the two databases individually. The results rejected (p

370   < 0.01) the null hypothesis that either ship or float pCO_2 follows a normal distribution. Consequently, we employed Mann-Whitney U Testing to evaluate the consistency between adjusted ship pCO_2 and float pCO_2 data (Supplement Fig. S10). These tests rejected (p < 0.01) the null hypothesis of no difference between ship and float data. Based on the outcomes of these hypothesis tests, it can be concluded that, even after accounting for all factors corrected, there still exists a significant offset between ship pCO_2 and float pCO_2. It should be noted that although we find discrepancies between average values, we

375   do not assert that all float-based pCO_2 data are erroneous; rather, our regional and overall assessments underscore the existence of uncertainties within the float data.

It is necessary to be aware that this final $\Delta pCO_{2,\text{Surface}}$ value may be an underestimate. The largest adjustment we applied (reducing $\Delta pCO_{2,\text{Surface}}$ by 24.4 µatm) was the normalization of pCO_2 to a reference year of 2005, to eliminate the impact of increasing anthropogenic carbon over time. This may, however, be an overcorrection, because it assumes that air-sea gas

380   exchange has run to completion in all surface waters. The equilibration of CO_2 is estimated to take many months in the SO (Jones et al., 2014); for this reason, it is likely that some surface waters were not at equilibrium at the time of measurement. The overall saturation level is difficult to quantify, but a modelling study suggests considerable deviations from saturation (Fig. 8(c) of Jones et al. (2014)). Widespread ocean-atmosphere imbalances would undoubtedly increase the value of the final discrepancy. Therefore, we consider our $\Delta pCO_{2,\text{Surface}}$ calculation of 9.4 µatm to be a conservative estimate.

385   **4.5 Implications**

Returning to our initial question, correctly defining pCO_2 at the sea surface is crucial in constraining the global oceanic carbon sink, making the $\Delta pCO_{2,\text{Surface}}$ parameter highly meaningful for CO_2 flux estimates. This result of a definite, non-negligible discrepancy has the following implications: (1) float-based pCO_2 estimates are biased high compared to other observations in the SO; (2) this bias can potentially explain the mismatch between float-based CO_2 air-sea flux estimates and

390   those from other sources (e.g. Long et al., 2021); (3) our analyses suggests that the overestimation of surface pCO_2 by floats could be roughly within the uncertainty estimate of Williams et al. (2017) of ±2.7% (i.e., ±11 µatm), although it could also be higher.

Such a high bias implies that the current calculation scheme for float pH and by extension pCO_2 has quality problems in agreement with (Wimart-Rousseau et al., 2023) and others. In order to maximize the utility of carbon measurements on

395   floats, a comprehensive reconsideration of all factors contributing to uncertainties in float pCO_2 is recommended. Williams et al. (2017) grouped sources of uncertainty in float pCO_2 values into three main categories: (1) pH sensors, (2) alkalinity estimates, and (3) carbonate system equilibrium constants. Future work should identify which out of these three categories is responsible for the majority of the pCO_2 biases and focus on reducing these uncertainties.

Gray et al. (2018) and Bushinsky et al., (2019) previously implemented adjustment to float pCO_2 corresponding to a 4 µatm

400   reduction across the Southern Ocean surface layer, considering the differences with nearby ship's data. Other studies (e.g.

Huang et al., 2023) did not implement an adjustment, following a recommendation by the U.S. Ocean Carbon and Biogeochemistry Program working group entitled the Ocean Carbonate System Intercomparison Forum (SI Appendix, Text S1.8) not to do so. Our results suggest that an adjustment should be applied, and that it should be larger than 4 μatm. The use of a 4 μatm reduction brought Gray et al.'s (2018) results closer to, albeit still significantly higher than, the flux calculated

405 from ship data and other database results (Long et al., 2021, Gray et al., 2018, Bushinsky et al., 2019). Considering the differences we have identified, the comprehensive adjustment of Southern Ocean float surface pCO$_2$ for the purpose of calculating air-sea flux is anticipated to yield a significantly greater CO$_2$ uptake estimate. Consequently, such an adjustment will most likely enhance the consistency of float calculations with other databases and promote a greater alignment of CO$_2$ flux estimates.

410 **5 Conclusions**

In this study, a significant inconsistency was found between float-based and ship-based pCO$_2$ in the Southern Ocean. Float pCO$_2$ values were found to be, on average, higher than ship pCO$_2$ values obtained at the same depths across the entire float profile. Supporting this conclusion, float pCO$_2$ also exhibits higher values overall when compared with oxygen relationships. Several alternative possible explanations were considered for the observed discrepancy in pCO$_2$: spatial sampling bias,

415 seasonal sampling bias, errors in TA, choice of carbonate system constants and higher levels of anthropogenic CO$_2$ in float data. These factors were found to change the value of the difference to some extent, but could not fully explain the observed discrepancy. Applying several corrections together left a discrepancy of 10 μatm in the top 100m, 7 μatm at depth. The conclusion is further supported by CORS analysis. Thus, we conclude that the pCO$_2$ discrepancies are due to float pCO$_2$ data quality issues. By incorporating this discrepancy to further refine the Southern Ocean surface pCO$_2$ data, a notable increase

420 in the estimated values of net air-sea CO$_2$ uptake is anticipated. This adjustment is expected to align the calculated flux results more closely with other independent datasets in Southern Ocean. Our results suggest that the calculation scheme of pCO$_2$ from float pH needs further refinement; all sources of uncertainty should be considered, in order to identify those processes that lead to the disparities obtained in this study. More accurate pCO$_2$ data derived from floats will be of great value in future analyses of Southern Ocean carbon uptake and release, and globally.

425

Code/Data Availability

All BGC-Argo data Data were collected and made freely available by the Global Ocean Biogeochemistry Array (GO-BGC)
435   Project funded by the National Science Foundation, Division of Ocean Sciences (NSF OCE-1946578), and by the
International Argo Program and the national programs that contribute to it. (http://www.argo.ucsd.edu, http://ocean-ops.org).
The Argo Program is part of the Global Ocean Observing System. The GLODAPv2.2022 dataset was downloaded from
https://glodap.info/.   The monthly mean atmospheric xCO_2 values for observing site were obtained from
ftp://aftp.cmdl.noaa.gov/data/trace_gases/co2/flask/.
440

Declaration of Competing Interest

The authors declare that they have no known competing financial interests or personal relationships that could have
appeared to influence the work reported in this paper.

445   **Author contribution**

C.Z. and T.T. conceived the original idea and came up with methods of research. C.Z. performed the analytic calculations,
coding and writing. T.T. supervised the project. Y.W, P.B., D.S. and A.S provided significant comments and help specific in
coding, calculating and Data collection.

450   **References**

ÁLVAREZ, M., FAJAR, N. M., CARTER, B. R., GUALLART, E. F., PéREZ, F. F., WOOSLEY, R. J. & MURATA, A.
        2020. Global ocean spectrophotometric pH assessment: consistent inconsistencies. *Environmental Science &
        Technology,* 54**,** 10977-10988.
BAKKER, D. C. E., PFEIL, B., LANDA, C. S., METZL, N., O'BRIEN, K. M., OLSEN, A., SMITH, K., COSCA, C.,
455   HARASAWA, S., JONES, S. D., NAKAOKA, S., NOJIRI, Y., SCHUSTER, U., STEINHOFF, T., SWEENEY, C.,
        TAKAHASHI, T., TILBROOK, B., WADA, C., WANNINKHOF, R., ALIN, S. R., BALESTRINI, C. F.,
        BARBERO, L., BATES, N. R., BIANCHI, A. A., BONOU, F., BOUTIN, J., BOZEC, Y., BURGER, E. F., CAI, W.
        J., CASTLE, R. D., CHEN, L., CHIERICI, M., CURRIE, K., EVANS, W., FEATHERSTONE, C., FEELY, R. A.,
        FRANSSON, A., GOYET, C., GREENWOOD, N., GREGOR, L., HANKIN, S., HARDMAN-MOUNTFORD, N.
460   J., HARLAY, J., HAUCK, J., HOPPEMA, M., HUMPHREYS, M. P., HUNT, C. W., HUSS, B., IBáNHEZ, J. S. P.,
        JOHANNESSEN, T., KEELING, R., KITIDIS, V., KöRTZINGER, A., KOZYR, A., KRASAKOPOULOU, E.,
        KUWATA, A., LANDSCHüTZER, P., LAUVSET, S. K., LEFèVRE, N., LO MONACO, C., MANKE, A.,
        MATHIS, J. T., MERLIVAT, L., MILLERO, F. J., MONTEIRO, P. M. S., MUNRO, D. R., MURATA, A.,
        NEWBERGER, T., OMAR, A. M., ONO, T., PATERSON, K., PEARCE, D., PIERROT, D., ROBBINS, L. L.,
465   SAITO, S., SALISBURY, J., SCHLITZER, R., SCHNEIDER, B., SCHWEITZER, R., SIEGER, R., SKJELVAN,
        I., SULLIVAN, K. F., SUTHERLAND, S. C., SUTTON, A. J., TADOKORO, K., TELSZEWSKI, M., TUMA, M.,
        VAN HEUVEN, S. M. A. C., VANDEMARK, D., WARD, B., WATSON, A. J. & XU, S. 2016. A multi-decade
        record of high-quality fCO2 data in version 3 of the Surface Ocean CO2 Atlas (SOCAT). *Earth Syst. Sci. Data,* 8**,**
        383-413.
470   BATES, N. R., ASTOR, Y. M., CHURCH, M. J., CURRIE, K., DORE, J. E., GONZáLEZ-DáVILA, M., LORENZONI, L.,
        MULLER-KARGER, F., OLAFSSON, J. & SANTANA-CASIANO, J. M. 2014. A time-series view of changing

surface ocean chemistry due to ocean uptake of anthropogenic CO_2 and ocean acidification. *Oceanography,* 27**,** 126-141.

BAUER, J. E., CAI, W.-J., RAYMOND, P. A., BIANCHI, T. S., HOPKINSON, C. S. & REGNIER, P. A. 2013. The
475   changing carbon cycle of the coastal ocean. *Nature,* 504**,** 61-70.

BITTIG, H. C., MAURER, T. L., PLANT, J. N., SCHMECHTIG, C., WONG, A. P., CLAUSTRE, H., TRULL, T. W., UDAYA BHASKAR, T., BOSS, E. & DALL'OLMO, G. 2019. A BGC-Argo guide: Planning, deployment, data handling and usage. *Frontiers in Marine Science,* 6**,** 502.

BUSHINSKY, S. M., LANDSCHüTZER, P., RöDENBECK, C., GRAY, A. R., BAKER, D., MAZLOFF, M. R.,
480   RESPLANDY, L., JOHNSON, K. S. & SARMIENTO, J. L. 2019. Reassessing Southern Ocean air-sea CO2 flux estimates with the addition of biogeochemical float observations. *Global Biogeochemical Cycles,* 33**,** 1370-1388.

CARTER, B., FEELY, R., WILLIAMS, N., DICKSON, A., FONG, M. & TAKESHITA, Y. 2018. Updated methods for global locally interpolated estimation of alkalinity, pH, and nitrate. *Limnology and Oceanography: Methods,* 16**,** 119-131.

485 CLAUSTRE, H., JOHNSON, K. S. & TAKESHITA, Y. 2020. Observing the global ocean with biogeochemical-Argo. *Annual review of Marine science,* 12**,** 23-48.

DE BOYER MONTéGUT, C., MADEC, G., FISCHER, A. S., LAZAR, A. & IUDICONE, D. 2004. Mixed layer depth over the global ocean: An examination of profile data and a profile-based climatology. *Journal of Geophysical Research: Oceans,* 109.

490 DONG, S., SPRINTALL, J., GILLE, S. T. & TALLEY, L. 2008. Southern Ocean mixed-layer depth from Argo float profiles. *Journal of Geophysical Research: Oceans,* 113.

FEELY, R. A., SABINE, C. L., HERNANDEZ-AYON, J. M., IANSON, D. & HALES, B. 2008. Evidence for upwelling of corrosive" acidified" water onto the continental shelf. *science,* 320**,** 1490-1492.

FRENZEL, H., SHARP, JONATHAN D., FASSBENDER, ANDREA J., & BUZBY, NINA. 2022. OneArgo-Mat: A
495   MATLAB toolbox for accessing and visualizing Argo data (v1.0.3). . *Zenodo.*

GARCIA & GORDON 1993. OXYGEN SOLUBILITY IN SEAWATER - BETTER FITTING EQUATIONS (VOL 37, PG 1308, 1992). *Limnology and Oceanography,* 38**,** 656-656.

GARCIA, H. E. & GORDON, L. I. 1992. OXYGEN SOLUBILITY IN SEAWATER - BETTER FITTING EQUATIONS. *Limnology and Oceanography,* 37**,** 1307-1312.

500 GRAY, A. R., JOHNSON, K. S., BUSHINSKY, S. M., RISER, S. C., RUSSELL, J. L., TALLEY, L. D., WANNINKHOF, R., WILLIAMS, N. L. & SARMIENTO, J. L. 2018. Autonomous biogeochemical floats detect significant carbon dioxide outgassing in the high-latitude Southern Ocean. *Geophysical Research Letters,* 45**,** 9049-9057.

GRUBER, N., LANDSCHüTZER, P. & LOVENDUSKI, N. S. 2019. The variable Southern Ocean carbon sink. *Annual review of marine science,* 11**,** 159-186.

505 HUANG, Y., FASSBENDER, A. J. & BUSHINSKY, S. M. 2023. Biogenic carbon pool production maintains the Southern Ocean carbon sink. *Proceedings of the National Academy of Sciences,* 120**,** e2217909120.

JOHNSON, K. S., PLANT, J. N., COLETTI, L. J., JANNASCH, H. W., SAKAMOTO, C. M., RISER, S. C., SWIFT, D. D., WILLIAMS, N. L., BOSS, E. & HAëNTJENS, N. 2017. Biogeochemical sensor performance in the SOCCOM profiling float array. *Journal of Geophysical Research: Oceans,* 122**,** 6416-6436.

510 JONES, D. C., ITO, T., TAKANO, Y. & HSU, W. C. 2014. Spatial and seasonal variability of the air-sea equilibration timescale of carbon dioxide. *Global Biogeochemical Cycles,* 28**,** 1163-1178.

LANDSCHüTZER, P., GRUBER, N., HAUMANN, F. A., RöDENBECK, C., BAKKER, D. C., VAN HEUVEN, S., HOPPEMA, M., METZL, N., SWEENEY, C. & TAKAHASHI, T. 2015. The reinvigoration of the Southern Ocean carbon sink. *Science,* 349**,** 1221-1224.

515 LAUVSET, S. K., LANGE, N., TANHUA, T., BITTIG, H. C., OLSEN, A., KOZYR, A., ALIN, S. R., ÁLVAREZ, M., AZETSU-SCOTT, K. & BARBERO, L. 2022. GLODAPv2. 2022: the latest version of the global interior ocean biogeochemical data product. *Earth System Science Data Discussions,* 2022**,** 1-37.

LAUVSET, S. K., LANGE, N., TANHUA, T., BITTIG, H. C., OLSEN, A., KOZYR, A., ÁLVAREZ, M., BECKER, S., BROWN, P. J. & CARTER, B. R. 2021. An updated version of the global interior ocean biogeochemical data
520   product, GLODAPv2. 2021. *Earth System Science Data,* 13**,** 5565-5589.

LENTON, A., TILBROOK, B., LAW, R. M., BAKKER, D., DONEY, S. C., GRUBER, N., ISHII, M., HOPPEMA, M., LOVENDUSKI, N. S. & MATEAR, R. J. 2013. Sea–air CO 2 fluxes in the Southern Ocean for the period 1990–2009. *Biogeosciences,* 10**,** 4037-4054.

LONG, M. C., STEPHENS, B. B., MCKAIN, K., SWEENEY, C., KEELING, R. F., KORT, E. A., MORGAN, E. J., BENT, J. D., CHANDRA, N. & CHEVALLIER, F. 2021. Strong Southern Ocean carbon uptake evident in airborne observations. *Science,* 374**,** 1275-1280.

LUEKER, T. J., DICKSON, A. G. & KEELING, C. D. 2000. Ocean pCO2 calculated from dissolved inorganic carbon, alkalinity, and equations for K1 and K2: validation based on laboratory measurements of CO2 in gas and seawater at equilibrium. *Marine chemistry,* 70**,** 105-119.

MACKAY, N. & WATSON, A. 2021. Winter air-sea CO2 fluxes constructed from summer observations of the polar southern ocean suggest weak outgassing. *Journal of Geophysical Research: Oceans,* 126**,** e2020JC016600.

MATSUMOTO, G. I., JOHNSON, K. S., RISER, S., TALLEY, L., WIJFFELS, S. & HOTINSKI, R. 2022. The Global Ocean Biogeochemistry (GO-BGC) Array of Profiling Floats to Observe Changing Ocean Chemistry and Biology. *Marine Technology Society Journal,* 56.

MAURER, T. L., PLANT, J. N. & JOHNSON, K. S. 2021. Delayed-mode quality control of oxygen, nitrate, and pH data on SOCCOM biogeochemical profiling floats. *Frontiers in Marine Science,* 8**,** 683207.

MCNEIL, B. I., METZL, N., KEY, R. M., MATEAR, R. J. & CORBIERE, A. 2007. An empirical estimate of the Southern Ocean air-sea CO2 flux. *Global Biogeochemical Cycles,* 21.

METZL, N., BRUNET, C., JABAUD-JAN, A., POISSON, A. & SCHAUER, B. 2006. Summer and winter air–sea CO2 fluxes in the Southern Ocean. *Deep Sea Research Part I: Oceanographic Research Papers,* 53**,** 1548-1563.

MUNRO, D. R., LOVENDUSKI, N. S., STEPHENS, B. B., NEWBERGER, T., ARRIGO, K. R., TAKAHASHI, T., QUAY, P. D., SPRINTALL, J., FREEMAN, N. M. & SWEENEY, C. 2015. Estimates of net community production in the Southern Ocean determined from time series observations (2002–2011) of nutrients, dissolved inorganic carbon, and surface ocean pCO2 in Drake Passage. *Deep Sea Research Part II: Topical Studies in Oceanography,* 114**,** 49-63.

OWENS, W. B., ZILBERMAN, N., JOHNSON, K. S., CLAUSTRE, H., SCANDERBEG, M., WIJFFELS, S. & SUGA, T. 2022. OneArgo: A New Paradigm for Observing the Global Ocean. *Marine Technology Society Journal,* 56.

PIERROT, D., NEILL, C., SULLIVAN, K., CASTLE, R., WANNINKHOF, R., LüGER, H., JOHANNESSEN, T., OLSEN, A., FEELY, R. A. & COSCA, C. E. 2009. Recommendations for autonomous underway pCO2 measuring systems and data-reduction routines. *Deep Sea Research Part II: Topical Studies in Oceanography,* 56**,** 512-522.

RAE, J. W., BURKE, A., ROBINSON, L., ADKINS, J. F., CHEN, T., COLE, C., GREENOP, R., LI, T., LITTLEY, E. & NITA, D. 2018. CO2 storage and release in the deep Southern Ocean on millennial to centennial timescales. *Nature,* 562**,** 569-573.

RINTOUL, S. R. 2011. The southern ocean in the earth system. *Science diplomacy: Antarctica, science, and the governance of international spaces*.

ROY, R. N., ROY, L. N., VOGEL, K. M., PORTER-MOORE, C., PEARSON, T., GOOD, C. E., MILLERO, F. J. & CAMPBELL, D. M. 1993. The dissociation constants of carbonic acid in seawater at salinities 5 to 45 and temperatures 0 to 45 C. *Marine Chemistry,* 44**,** 249-267.

SCHMECHTIG, C. & THIERRY, V. 2016. Argo quality control manual for biogeochemical data.

SHARP, J. D., PIERROT, DENIS, HUMPHREYS, MATTHEW P., EPITALON, JEAN-MARIE, ORR, JAMES C., LEWIS, ERNIE R., & WALLACE, DOUGLAS W.R. 2023. CO2SYSv3 for MATLAB (v3.2.1). *Zenodo.*

SULPIS, O., LAUVSET, S. K. & HAGENS, M. 2020. Current estimates of K 1* and K 2* appear inconsistent with measured CO 2 system parameters in cold oceanic regions. *Ocean Science,* 16**,** 847-862.

SUTTON, A. J., WILLIAMS, N. L. & TILBROOK, B. 2021. Constraining Southern Ocean CO2 flux uncertainty using uncrewed surface vehicle observations. *Geophysical Research Letters,* 48**,** e2020GL091748.

TAKAHASHI, T., SUTHERLAND, S. C., CHIPMAN, D. W., GODDARD, J. G., HO, C., NEWBERGER, T., SWEENEY, C. & MUNRO, D. 2014. Climatological distributions of pH, pCO2, total CO2, alkalinity, and CaCO3 saturation in the global surface ocean, and temporal changes at selected locations. *Marine Chemistry,* 164**,** 95-125.

VAN HEUVEN, S., PIERROT, D., RAE, J., LEWIS, E. & WALLACE, D. 2011. MATLAB program developed for CO2
570   system calculations. *ORNL/CDIAC-105b. Carbon Dioxide Information Analysis Center, Oak Ridge National
         Laboratory, US Department of Energy, Oak Ridge, Tennessee,* 530.
WEISS, R. & PRICE, B. 1980a. Nitrous oxide solubility in water and seawater. *Marine chemistry,* 8**,** 347-359.
WEISS, R. F. 1974. Carbon dioxide in water and seawater: the solubility of a non-ideal gas. *Marine chemistry,* 2**,** 203-215.
WEISS, R. F. & PRICE, B. A. 1980b. NITROUS-OXIDE SOLUBILITY IN WATER AND SEAWATER. *Marine
575   Chemistry,* 8**,** 347-359.
WILLIAMS, N., JURANEK, L., FEELY, R., JOHNSON, K., SARMIENTO, J. L., TALLEY, L., DICKSON, A., GRAY, A.,
         WANNINKHOF, R. & RUSSELL, J. 2017. Calculating surface ocean pCO2 from biogeochemical Argo floats
         equipped with pH: An uncertainty analysis. *Global Biogeochemical Cycles,* 31**,** 591-604.
WIMART-ROUSSEAU, C., STEINHOFF, T., KLEIN, B., BITTIG, H. & KöRTZINGER, A. 2023. Enhancement of float-
580   pH data quality control methods: A study case in the Subpolar Northwestern Atlantic region. *Biogeosciences
         Discussions,* 2023**,** 1-26.
WOOSLEY, R. J. & MOON, J.-Y. 2023. Re-evaluation of carbonic acid dissociation constants across conditions and the
         implications for ocean acidification. *Marine Chemistry***,** 104247.
WU, Y., BAKKER, D. C., ACHTERBERG, E. P., SILVA, A. N., PICKUP, D. D., LI, X., HARTMAN, S., STAPPARD, D.,
585   QI, D. & TYRRELL, T. 2022. Integrated analysis of carbon dioxide and oxygen concentrations as a quality control
         of ocean float data. *Communications Earth & Environment,* 3**,** 92.
WU, Y., HAIN, M. P., HUMPHREYS, M. P., HARTMAN, S. & TYRRELL, T. 2019. What drives the latitudinal gradient in
         open-ocean surface dissolved inorganic carbon concentration? *Biogeosciences,* 16**,** 2661-2681.
WU, Y. & QI, D. 2022. Inconsistency between ship-and Argo float-based p CO 2 at the intense upwelling region of the
590   Drake Passage, Southern Ocean. *Frontiers in Marine Science,* 9.
WU, Y. & QI, D. 2023. The controversial Southern Ocean air-sea CO2 flux in the era of autonomous ocean observations.
         *Science Bulletin***,** S2095-9273 (23) 00615.